Journal of Materials Chemistry B

Accepted Manuscript

This is an *Accepted Manuscript*, which has been through the Royal Society of Chemistry peer review process and has been accepted for publication.

Accepted Manuscripts are published online shortly after acceptance, before technical editing, formatting and proof reading. Using this free service, authors can make their results available to the community, in citable form, before we publish the edited article. We will replace this *Accepted Manuscript* with the edited and formatted *Advance Article* as soon as it is available.

You can find more information about *Accepted Manuscripts* in the Information for Authors.

Please note that technical editing may introduce minor changes to the text and/or graphics, which may alter content. The journal's standard Terms & Conditions and the Ethical guidelines still apply. In no event shall the Royal Society of Chemistry be held responsible for any errors or omissions in this *Accepted Manuscript* or any consequences arising from the use of any information it contains.

ROYAL SOCIETY OF CHEMISTRY

www.rsc.org/materialsB

Journal of Materials Chemistry B

PAPER

Glutamine-chitosan modified calcium phosphate nanoparticles for efficient siRNA delivery and osteogenic differentiation

Received 00th January 20xx,
Accepted 00th January 20xx

DOI: 10.1039/x0xx00000x

www.rsc.org/

Bogyu Choi,[a,†] Zhong-Kai Cui,[a,†] Soyon Kim,[b] Jiabing Fan,[a] Benjamin M. Wu[a,b] and Min Lee[a,b,*]

RNA interference (RNAi)-based therapy using small interfering RNA (siRNA) exhibits great potential to treat diseases. Although calcium phosphate (CaP)-based systems are attractive options to deliver nucleic acids due to their good biocompatibility and high affinity with nucleic acids, they are limited by uncontrollable particle formation and inconsistent transfection efficiencies. In this study, we developed a stable CaP nanocarrier system with enhanced intracellular uptake by adding highly cationic, glutamine-conjugated oligochitosan (Gln-OChi). CaP nanoparticles coated with Gln-OChi (CaP/Gln-OChi) significantly enhanced gene transfection and knockdown efficiency in both immortalized cell line (HeLa) and primary mesenchymal stem cells (MSCs) with minimal cytotoxicity. The osteogenic bioactivity of siRNA-loaded CaP/Gln-OChi particles was further confirmed in three-dimensional environments by using photocrosslinkable chitosan hydrogels encapsulating MSCs and particles loaded with siRNA targeting noggin, a bone morphogenetic protein antagonist. These findings suggest that our CaP/Gln-OChi nanocarrier provides an efficient and safe gene delivery system for therapeutic applications.

Introduction

Gene therapy has been extensively investigated to treat diseases by delivering nucleic acids into cells to induce or silence specific gene expression.[1-3] In particular, RNA interference (RNAi)-based therapy, mediated by small interfering ribonucleic acids (siRNA), exhibits great potential for cancer treatment[4] or tissue engineering applications by suppressing expression of a gene of interest and directing cell behaviors.[5] Given that naked siRNA scarcely has cellular penetration due to its large size and anionic nature, various carriers have been developed for efficient delivery of siRNA.[6-10] Although viral vectors provide highly efficient gene transfer in genetic engineering of cells,[11] the risk of viral insertional mutagenesis and immunogenicity limits their clinical potential.[12-14] Therefore, non-viral delivery systems have been investigated to transfer siRNA in a safe and efficient manner.[5, 8, 13]

Calcium phosphate (CaP) precipitates have been utilized as DNA transfer vehicles to mammalian cells for a long time due to their good biocompatibility, high affinity with DNA, ease of use and cost-efficiency.[15-21] In addition, CaP occurs as natural bone mineral and its pH-dependent solubility enables release of encapsulated nucleic acids into the cytoplasm by endosomal acidification.[21, 22] These characteristics make CaP an attractive option to deliver nucleic acids.[21-24] However, a major drawback of current CaP-based carriers is their inconsistent transfection efficiencies. This is mainly due to their uncontrollable particle size and formation of large aggregates during rapid CaP precipitation.[25]

Cell-based therapy using stem or progenitor cells with their genetic modification is an attractive option to regenerate damaged tissues and treat various diseases. In particular, mesenchymal stem cells (MSCs) are promising candidates for clinical applications due to their ability to be expanded to large cell numbers and differentiated into various cell lineages.[26-28] Non-viral gene delivery was efficient at transferring genes into cancer cells or other fast dividing cell lines, but less effective at transferring genes to MSCs or primary cells.[29-31] Thus, investigations have been exploited to stabilize CaP colloidal systems to increase its transfection efficiency.[22, 25]

In this study, we developed a strategy to stabilize the formation of CaP particles and enhance their cellular uptake for efficient delivery of siRNA molecules using glutamine (Gln)-conjugated oligochitosan (OChi). Chitosan is a naturally occurring polysaccharide and is widely used in biomedical applications due to its biocompatibility, biodegradability, and low immunogenicity.[32-34] Moreover, abundant primary amine groups in chitosan facilitate the formation of electrostatic complexes with negatively charged siRNA. Chitosan derivatives such as OChi exhibit lower viscosity and higher solubility at physiological pH than chitosan, making them more attractive to be applied in biomedical formulations. It has been demonstrated that positive surface charges induced a great binding with genes and enhanced cellular uptake of the

[a] Division of Advanced Prosthodontics, University of California Los Angeles, 10833 Le Conte Avenue, Los Angeles, California 90095, USA. Email: leemin@ucla.edu
[b] Department of Bioengineering, University of California Los Angeles, 410 Westwood Plaza, Los Angeles, California 90095, USA.
† Co-first author: These authors contributed equally to this work.
‡ Electronic Supplementary Information (ESI) available. See DOI: 10.1039/x0xx00000x

This journal is © The Royal Society of Chemistry 20xx

Journal of Materials Chemistry B Accepted Manuscript

Please do not adjust margins

nanoparticles.[35-38] We further modified OChi using highly cationic Gln (pKa = 9.13) to create a particle with high net positive charge under normal physiological conditions (pH = 7.4). We evaluated the transfection and gene silencing efficiency of the CaP particles modified with Gln-conjugated OChi (CaP/Gln-OChi) in both HeLa cells and adipose-derived MSCs (ADSCs) expressing green fluorescent proteins (GFP). We further investigated the feasibility of the CaP/Gln-OChi particles to induce osteogenic differentiation of MSCs by loading Noggin targeting siRNA (siNOG) into the particles and subsequently embedding them into three-dimensional (3D) hydrogels with ADSCs.

Experimental

Synthesis of Gln-OChi

Gln-OChi was synthesized using EDC chemistry.[39] Briefly, Gln (Invitrogen, Carlsbad, CA) was added at a concentration of 5% (w/v) to OChi (Mw 5 kDa, 86% deacetylated, Sigma-Aldrich, St. Louis, MO) aqueous solution (1% (w/v)) under stirring. To this solution, EDC (Sigma-Aldrich) was added drop wise at a final concentration of 0.1 M. The reaction was continued for 15 h and the resultant solution was dialyzed against distilled water with four changes, subsequently lyophilized and stored at 4 ^{o}C. The substitution degree of Gln (DSGln) in Gln-OChi was assessed using ^{1}H NMR (D_2O for Gln and OChi, D_2O/acetic acid for Gln-OChi).

Preparation of Gln-OChi coated CaP nanoparticles incorporating siRNA

siRNA-loaded CaP particles were prepared as described previously[40] with some modifications. Briefly, a solution of 2.5 M $CaCl_2$ was diluted in 10 mM Tris/HCl buffer (pH 7.5) (2 : 23 µL) (solution A). Another solution (10 µL) of 50 mM Hepes buffer containing 1.5 mM Na_3PO_4 and 140 mM NaCl (pH 7.5) was mixed with siRNA (10 µM, 10 µL) (solution B). Solution A was mixed with solution B by short vortex. Chitosan (OChi or Gln-OChi) solution (0.02% w/v, pH 6, 35 µL) was subsequently added during vortex mixing (1,500 rpm) at a weight ratio of 5 to siRNA. The pH of the final reaction solution was approximately 7. Commercially available Lipofectamine® 2000 (Invitrogen, Carlsbad, CA) was used as a positive control. Lipoplexes were prepared as described in the manufacturer's protocol at a Lipofectamine® 2000/siRNA weight ratio of 7.5. Each sample solution was used immediately after preparation. Chitosan NPs incorporating siRNA without CaP (OChi/siRNA or Gln-OChi/siRNA) were prepared at a weight ratio of 50 as previously described.[41, 42] The incorporation efficiency (%) of siRNA in the particles was determined using fluorescently labeled siRNA (Cy3-siRNA, Ambion Inc., Austin, TX). After Cy3-siRNA was loaded with the particles as stated above, particles were centrifuged at 13,000 rpm for 40 min, and then the amount of residual Cy3-siRNA in the supernatant was measured using fluorescent microplate reader (n = 3). The incorporation efficiency (%) was calculated using the following Equation:

$$\text{Incorporation efficiency}\ (\%) = \frac{T-S}{T} \times 100\% \qquad (1)$$

, where T is the total Cy3-siRNA and S is the amount of free Cy3-siRNA in the supernatant.

Characterization of nanoparticles

To observe morphology of particles, a drop of each particle-dispersed solutions as stated in section 4.2 was placed on silicon wafer and air-dried for 24 h, and then scanning electron microscopy (SEM; Nova NanoSEM230, FEI, Hillsboro, OR) was performed in low vacuum mode. The particle size was measured immediately after preparation and after incubation for 0.5, 1, 2, 3, and 20 h, respectively. The size and zeta-potential of particles were determined using Zetasizer Nano ZS (Malvern Instruments, Malvern, UK) (n = 3). Measurements were performed in water at an angle of 173^{o} and 25 ^{o}C.

Cell culture

HeLa cell line and eGFP expressing HeLa cell line (HeLa-GFP) were kind gifts from Dr. Kamei, University of California, Los Angeles. HeLa and HeLa-GFP cell lines were grown in the basal culture medium of Dulbecco's Modified Eagle's Medium (DMEM) supplemented with 10% fetal bovine serum (FBS), 100 U/mL penicillin/streptomycin. ADSCs and eGFP expressing ADSCs (ADSC-GFP) were isolated from inguinal fat pads in C57BL/6 mice at age of 4 - 8 weeks according to methods previously described.[43, 44] Briefly, adipose tissues collected from mice were washed in sterilized phosphate-buffered saline (PBS); cut into small pieces and digested with collagenase type I (0.1% w/v in PBS) for 2 h. The digested solution was centrifuged at 1,200 rpm for 5 min to collect cells, and then cell-pellet was resuspended in the basal culture medium. The resuspended cells were seeded onto tissue culture flasks.

Cytotoxicity assay

Cytotoxicity of nanoparticles was determined by alamarBlue assay (Invitrogen, Carlsbad, CA). Briefly, HeLa cell line or ADSCs were seeded in 96-well plates at a density of 3 x 10^4 cells/well or 1 x 10^4 cells/well, respectively. After 24 h incubation, medium was replaced by 100 µL transfection medium (DMEM medium containing 10% FBS) with various concentrations of nanoparticles and incubated for another 5 h for HeLa cell line and 15 h for ADSCs. Then, the medium was replaced with 100 µL of 10% (v/v) alamarBlue solution in basal medium. After 3 h incubation, the fluorescence intensity (FI) of alamarBlue was assayed at 600 nm (emission) with an excitation wavelength of 535 nm. Cells without nanoparticles (blank group) were taken as positive controls with 100% viability. As an untreated group, the 10% (v/v) alamarBlue solution was added in an empty well without cells and incubated together. The relative cell viability (%) was calculated using the following Equation:

$$\text{Relative cell viability}\ (\%) = \frac{FI_S - FI_{untreated}}{FI_{blank} - FI_{untreated}} \times 100\% \qquad (2)$$

, where FI_S, $FI_{untreated}$, and FI_{blank} are fluorescence intensity of sample, untreated group, and blank group, respectively.

Journal of Materials Chemistry B Accepted Manuscript

This journal is © The Royal Society of Chemistry 20xx

Please do not adjust margins

Cellular uptake and GFP silencing studies in 2D monolayer cultures

HeLa cell line or ADSCs were seeded onto 8-well chambered glass for 2D cellular uptake study. For GFP silencing study, HeLa-GFP or ADSC-GFP was used. When cells were grown to 70% confluence, the basal growth medium was changed with the transfection medium. The cells were then incubated with the transfection media containing siRNA incorporated NPs for 6 h for HeLa cells or 15 h for ADSCs in a 37 ^{o}C humidified atmosphere with 5% CO_2. Fluorescently labeled siRNA (Cy3-siRNA) was used for cellular uptake study and anti-GFP siRNA (siGFP) (Life Technologies, Grand Island, NY) was used for GFP silencing study. Following this incubation, the media was aspirated and the cells were washed with PBS to remove any free-floating NPs. Then, cells were fixed with 10% neutral buffered formalin (NBF) solution and fluorescence images were observed using an Olympus IX71 microscope (Olympus, Tokyo, Japan). Transfection efficiency (%) was analyzed by counting transfected cells in relation to the total number of cells (n = 5).[45] Relative GFP intensity (%) was quantified by using NIH-ImageJ software (http:/rsb.info.nih.gov/ij/) and normalized by total cell number as determined by the DAPI staining (n = 5).

Cellular uptake in 3D hydrogels

Cy3-siRNA was incorporated into CaP/Gln-OChi to visualize cellular uptake of NPs inside hydrogel. Photocrosslinkable methacrylated glycol chitosan (MeGC) was prepared as previously described.[46] Mix ADSCs at a density of 2 x 10^6 cells/mL and CaP/Cy3-siRNA/Gln-OChi (final concentration of 625 nM for siRNA) in MeGC solution (final concentration of 2% w/v). The hydrogel was formed by exposing 40 µL of the solution to visible blue-light (400 - 500 nm, 500 - 600 mW/cm^2, Bisco Inc., Schaumburg, IL) in the presence of riboflavin (final concentration 6 µM), as a photoinitiator. Prepared hydrogels were incubated in 1 mL of transfection media for each time point. Following this incubation, the hydrogel was fixed with 10% NBF solution and images were taken using an Olympus IX71 microscope. Transfection efficiency (%) was quantified by counting transfected cells in relation to the total number of cells (n = 5).[45]

Noggin suppression in 3D hydrogels

siNOG incorporated CaP/Gln-OChi nanoparticles (CaP/siNOG/Gln-OChi) were prepared and encapsulated with ADSCs in MeGC hydrogels as described above. After 24 h of transfection, total RNA was extracted from the sample following the protocol developed by Flynn with a few modifications using TRIZOL (Invitrogen, Carlsbad, CA) and RNeasy Mini kit (Qiagen, Valencia, CA).[47] Total RNA was reverse transcribed to cDNA using cDNA transcription kit (Invitrogen, Carlsbad, CA). NOG expression was evaluated by quantitative real-time PCR using LightCycler 480 PCR system (Roche, Indianapolis, IN) with SYBR Green (n = 3). The housekeeping gene (GAPDH) expression was used to normalize NOG gene expression levels. The following primers were used. GAPDH: TGTGTCCGTCGTGGATCTGA (forward), CCTGCTTCACCACCTTCTTGA (reverse); NOG: GCCAGCACTATCTACACATCC (forward), GCGTCTCGTTCAGATCCTTCTC (reverse).

Osteogenic activity in 3D hydrogels

CaP/siNOG/Gln-OChi was encapsulated with ADSCs in MeGC hydrogels. After 24 h of transfection, transfection medium was replaced by osteogenic medium (basal medium supplemented with 50 µg/mL L-ascorbic acid, 10 mM glycerophosphate, 100 nM dexamethasone, and 100 ng/mL BMP2) and cultured for 3 days. Osteogenic differentiation was confirmed using alkaline phosphatase (ALP) staining and ALP activity assay. ALP staining was performed as previously described.[48] Briefly, cells were fixed in 10% NBF for 20 min, washed with PBS, and incubated in a solution consisting of Nitro Blue Tetrazolium (Sigma, St. Louis, MO) and 5-Brom-4-chlor-3-indoxylphosphat (Sigma, St. Louis, MO) stock solutions in AP buffer (100 mM Tris, 50 mM $MgCl_2$, 100 mM NaCl, pH 8.5) for 2 h. Macroscopic images were taken using Olympus SZX16 Stereomicroscope and magnified images were observed using an Olympus IX71 microscope. ALP expression appeared in blue. For ALP activity assay, samples were washed with PBS, incubated in a lysis buffer consisting of 0.01% Tween-20 diluted in PBS at 4 ^{o}C for 5 min. ALP activity was determined colorimetrically using p-nitrophenol phosphate (Sigma, St. Louis, MO) as a substrate and measured at 405 nm. Measurements were performed in triplicates and normalized to total protein contents determined by the MicroBCA protein assay kit (Thermo Scientific, Rockford, IL).

Statistical analysis

Statistical analysis was performed using the analysis of variances (ANOVA) followed by Tukey's post hoc test. A value of $p < 0.05$ was considered as significant.

Results and discussion

Nanoparticle preparation and characterization

Gln was covalently conjugated to OChi by EDC mediated chemical conjugation to increase its amino group content (Figure 1a). ^{1}H NMR spectra clearly showed the presence of Gln peaks at around 2.5 ppm and 2.2 ppm in the Gln-OChi, which were not detected in OChi. The DSGln was assessed by integration of the peaks at δ2.0 - 2.5 (-NH(CO)CH_3 of acetyl in OChi and -CH_2CH_2(CO)NH_2 of Gln) and δ2.9 - 3.2 (protons at the C2 position in OChi) (Figure 1b). The DSGln and the molecular weight of Gln-OChi determined by ^{1}H NMR were 9% and 5.4 kDa, respectively.

siRNA-loaded CaP nanoparticles (NPs) with (CaP/siRNA/OChi, CaP/siRNA/Gln-OChi) or without (CaP/siRNA) chitosan coating were prepared to examine the effects of Gln-OChi on NP formation and characteristics as illustrated in Figure 2a. The hydrodynamic size and zeta potential of particles were analyzed using Zetasizer Nano ZS. The initial mean diameter of CaP/siRNA NPs was 443 nm with a broad size distribution (PDI = 0.863). The addition of OChi or Gln-OChi significantly reduced the particle size to 89 nm or 119 nm, with a reduced PDI of 0.153 or 0.216, respectively. It is known that particles in size ranging from tens to one hundred nanometers are optimal for efficient endocytic uptake.[49] siNRA-loaded CaP precipitates rapidly formed large aggregates (~1.5 µm in diameter) in 1 h

Journal of Materials Chemistry B Accepted Manuscript

Please do not adjust margins

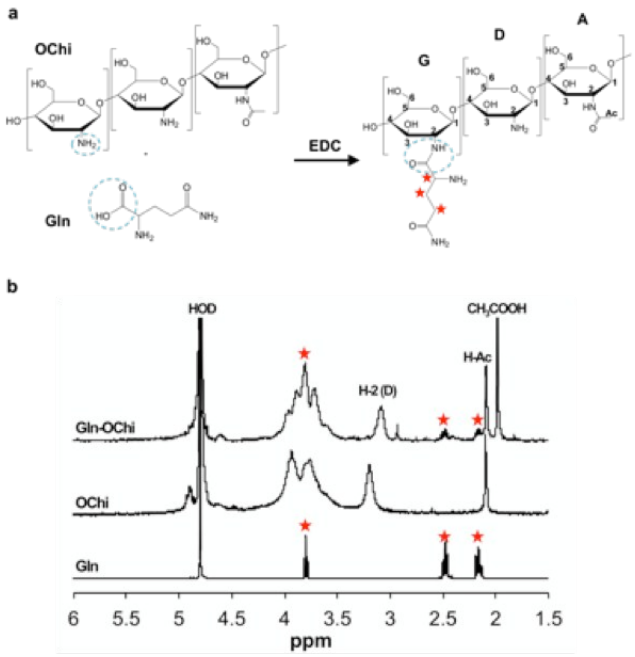

Figure 1. a) Synthesis of glutamine-graft-oligo-chitosan (Gln-OChi). b) ^{1}H NMR spectra of Gln-OChi, OChi, and Gln.

incubation at room temperature, while chitosan-modified CaP NPs were stable in dispersion for 24 h with a diameter of 110 nm and 172 nm for CaP/siRNA/OChi and CaP/siRNA/Gln-OChi, respectively (Figure 2b). The zeta potential of CaP/siRNA NPs was +13.0 ± 1.3 mV, while the modification of the particles with OChi or Gln-OChi greatly increased the zeta potentials to +32.3 ± 0.9 mV or +41.9 ± 1.2 mV, respectively. These results indicate that chitosan coating enhanced the surface charge and prevented particle aggregation because of electrostatic repulsion. In general, particles are physically stable when their zeta potential values are higher than 30 mV, while lower zeta potential values can lead to unstable particle dispersion.[50] The SEM observations revealed that chitosan-coated NPs are relatively spherical, while unmodified CaP/siRNA particles without chitosan coating formed large agglomerates during preparation (Figure 2c).

Although positive surface charge can improve cellular uptake, meanwhile it may present greater cytotoxicity.[41, 42, 51] The cytotoxicity of siRNA-loaded NPs was evaluated in HeLa cell line and primarily harvested ADSCs using an alamarBlue assay (Figure 3). CaP-based NPs with or without chitosan modification (CaP/siRNA/OChi, CaP/siRNA/Gln-Ochi, and CaP/siRNA) were found to be minimally cytotoxic and no significant decrease on cell viability was observed for both HeLa cells and ADSCs. Chitosan-based NPs (OChi/siRNA and Gln-OChi/siRNA) without CaP also displayed minimal cytotoxicity (Figure S1).

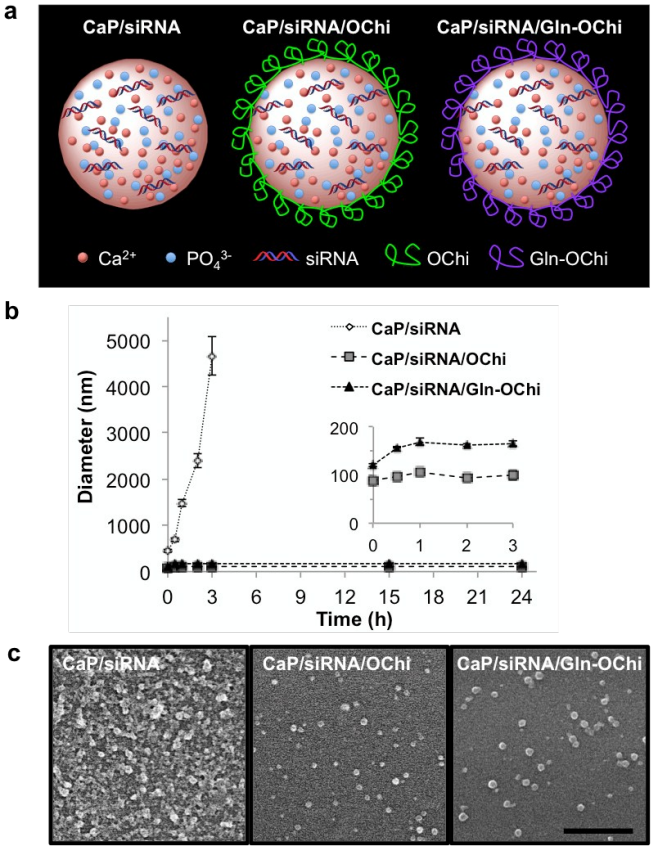

Figure 2. Characterization of siRNA-loaded CaP based NPs. a) Schematic illustration of siRNA-loaded CaP based NPs. b) Colloidal stability of siRNA-loaded CaP based NPs in distilled water as a function of time (n = 3). c) SEM images of siRNA-loaded CaP based NPs. Scale bar is 1 μm.

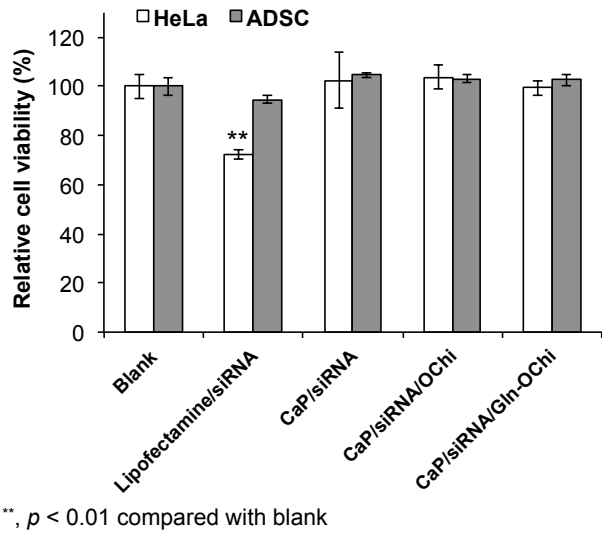

Figure 3. Cytotoxicity assay for Lipofectamine®/siRNA, siRNA-loaded CaP based NPs (CaP/siRNA, CaP/siRNA/OChi, and CaP/siRNA/Gln-OChi) evaluated in HeLa cell line and primarily harvested ADSCs using an alamarBlue assay.

Journal of Materials Chemistry B Accepted Manuscript

This journal is © The Royal Society of Chemistry 20xx

Please do not adjust margins

Cellular uptake and gene knockdown

The siRNA incorporation efficiency was found to be 80 ~ 83% for CaP related NPs used in this study, and 68% for Lipofectamine® 2000.

HeLa cell line. To test the potential of the NPs for intracellular delivery, HeLa cells were incubated with NPs containing fluorescently labeled model siRNA (Cy3-siRNA) for 6 h. Fluorescent microscopic observation showed that fluorescence was detected in the cells treated with NPs but not in the cells treated with free siRNA or blank NPs (Figure 4a). The transfection efficiency of CaP NPs was greatly increased from 65 ± 4% to 80 ± 2% after OChi modification (Figure 4b). Modification of CaP NPs with Gln-OChi further increased the transfection efficiency to 91 ± 6%, which was comparable to the Lipofectamine® 2000-mediated transfection (98 ± 3%). These data indicate that particle surface charges played a dominant role in membrane penetration and cellular internalization. The observed higher transfection efficiency may be attributed to the increased positive charge of the particles by chitosan or Gln moiety. It is well known that

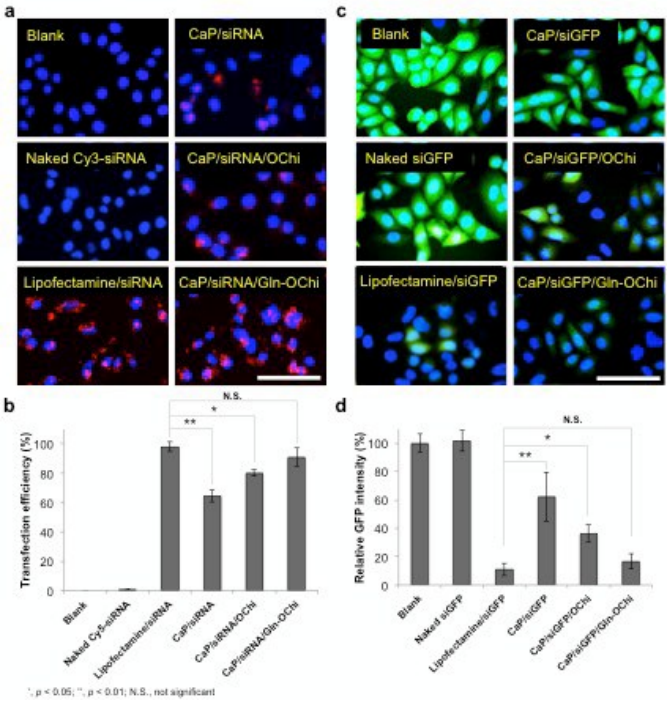

Figure 4. Effects of chitosan coating on transfection efficiency and knockdown efficiency in HeLa cell line. a) Cellular uptake of Cy3-siRNA-loaded NPs was observed using fluorescent microscopy after 6 h of transfection. Nuclei were counterstained with DAPI (blue). b) Transfection efficiency (%) of NPs into HeLa cell line was analyzed by counting transfected cells in relation to the total number of cells (n = 5). c) GFP silencing in HeLa-GFP was observed by fluorescent microscopy. d) Relative GFP silencing efficacy of NPs in HeLa-GFP was analyzed using ImageJ. Images are representative of a total analysis five samples. Scale bars are 100 µm.

positively charged particles can facilitate the nonspecific attachment to the negatively charged cellular membranes and promote subsequent uptake by cells.[52] It has been demonstrated that the particles with higher positive charges possessed stronger affinity with negatively charged proteoglycans of cell membrane, which led to higher cellular internalization.[35-38] It was also reported that the covalent conjugation of Gln to chitosan increased the mucoadhesivity and permeation capacity across intestinal tissue.[39, 53]

To determine the gene knockdown efficiency, NPs were loaded with GFP targeting siRNA (siGFP) and incubated with HeLa cells expressing GFP (Figure 4c and d). CaP-based NPs greatly suppressed the expression of GFP with the highest GFP suppression (83% ± 5%) from CaP/siGFP/Gln-OChi NPs, which was comparable to GFP suppression mediated by Lipofectamine® (89% ± 4%). No significant GFP suppression was observed in cells treated with free siGFP or blank NPs. These results indicate that increased surface charges by the chitosan modification induced a stable suspension of the NPs via electrostatic stability and improved cellular transfection efficiency, thus enhancing target gene silencing in HeLa cells. Since the chitosan NPs without CaP displayed strong positive charge of +27 - +29 mV (Table S1), their transfection efficiency were evaluated as well. The transfection efficiency of chitosan based NPs was 64 ± 2% and 84 ± 7% for OChi/Cy3-siRNA and Gln-OChi/Cy3-siRNA NPs, respectively, which was similar to those observed with CaP/Cy3-siRNA/OChi and CaP/Cy3-siRNA/Gln-OChi (Figure S2). However, the gene knockdown efficiency was significantly lower with the chitosan-based NPs compared with CaP-based NPs (Figure S3). Although positively charged surface of NPs facilitated cellular uptake in a charge dependent manner, these results indicate that the increased transfection efficiency does not necessarily lead to higher knockdown efficiency. The possible reasons could be that rapid dissociation of the ploylex before lysosome escape for low deacetylate chitosan and highly stable and inefficient polyplex formed by high deacetylate chitosan which did not dissociate after 24 h.[54, 55] The relative low gene knockdown efficiency of our chitosan-based NPs probably resulted from the high deacetylate chitosan used in the present study.

Primary ADSCs. Non-viral mediated gene delivery methods are often less efficient in primary cells. However, primary cells will be more clinically relevant in tissue engineering than immortalized cells. We verified the transfection efficiency and gene knockdown efficiency of the NPs using primary ADSCs. The transfection efficiency of Cy3-siRNA-loaded CaP was 28 ± 8% in ADSCs (Figure 5a and b), which was significantly lower ($p < 0.01$) than that in HeLa cell line (65 ± 4%). In contrast, CaP NPs modified with chitosan showed efficient cellular uptake in ADSCs, which was comparable to that observed in HeLa cell line. Specifically, the transfection efficiency was 73 ± 6% or 87 ± 5% with CaP/Cy3-siRNA/OChi or CaP/Cy3-siRNA/Gln-OChi NPs, respectively.

We also examined the GFP knockdown efficiency of the NPs in ADSC expressing GFP (Figure 5c and d). As expected, CaP/siGFP showed lower GFP silencing in ADSCs compared to HeLa cells. However, chitosan-modified CaP NPs (CaP/Cy3-siRNA/OChi or CaP/Cy3-siRNA/Gln-OChi) revealed similar GFP-silencing efficiency in primary ADSCs to that in HeLa cell line. This result is consistent with previous studies demonstrating that the transfection through nonviral vectors was less efficient in primary cells.[29-31] These results also indicate that sophisticated controls in sizes and surface charge density of NPs are required for effective gene transfection in primary cells.

Journal of Materials Chemistry B Accepted Manuscript

Please do not adjust margins

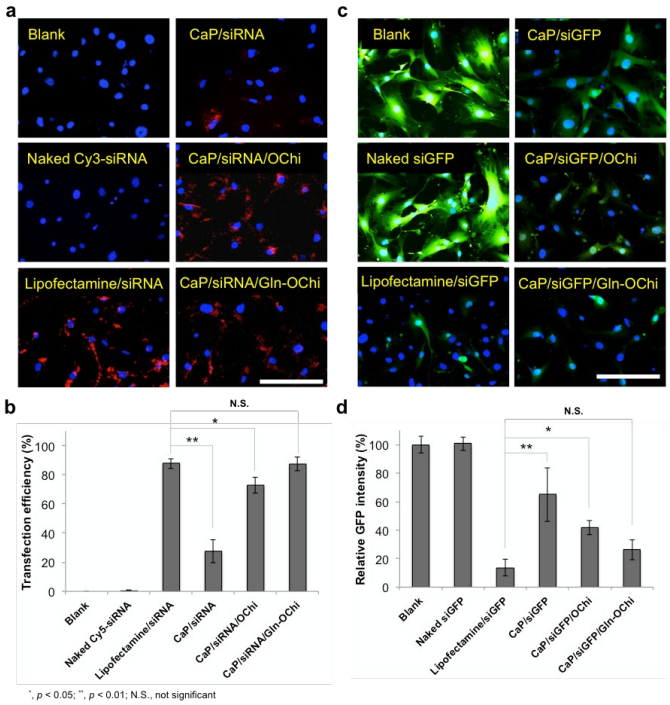

Figure 5. Effects of chitosan coating on transfection efficiency and knockdown efficiency in primarily harvested ADSCs. a) Cellular uptake of Cy3-siRNA-loaded NPs was observed using fluorescent microscopy after 6 h of transfection. Nuclei were counterstained with DAPI (blue). b) Transfection efficiency (%) of NPs into ADSCs was analyzed by counting transfected cells in relation to the total number of cells (n = 5). c) GFP silencing in ADSC-GFP was observed by fluorescent microscopy. d) Relative GFP silencing efficacy of NPs in ADSC-GFP was analyzed using ImageJ. Images are representative of a total analysis five samples. Scale bars are 100 µm.

Bioactivity of nanoparticles in 3D hydrogels

To investigate the feasibility of CaP/Gln-OChi NPs as an efficient gene carrier for bone tissue engineering, we evaluated the NPs in in vitro 3D setting by loading siRNA into the NPs and subsequently embedded them into photocrosslinkable chitosan hydrogels with ADSCs. We have previously developed the injectable hydrogel system using visible blue-light inducible chitosan (MeGC) and riboflavin initiator that supported proliferation and osteo- or chondrogenic differentiation of encapsulated MSCs.[46, 56, 57] Localization of siRNA-loaded NPs into the cells encapsulated in the hydrogel was visualized by incorporating fluorescent model siRNA (Cy3-siRNA) into the NPs (Figure 6). Fluorescent microscopy showed that the Cy3-siRNA loaded NPs were rapidly localized to the cells over time and cellular uptake was reached up to 85% after 24 h of incubation in the hydrogels (Figure 6b).

We further evaluated bioactivity of the NPs in the 3D hydrogel system by loading siNOG into CaP/Gln-OChi NPs. NOG is a specific antagonist of bone morphogenetic proteins (BMPs) and prevents BMPs from binding to their cell surface.[58-60] Our previous studies demonstrated that knockdown of NOG expression enhanced osteogenesis in vitro[48] and bone formation in vivo.[44] The expression of NOG mRNA was

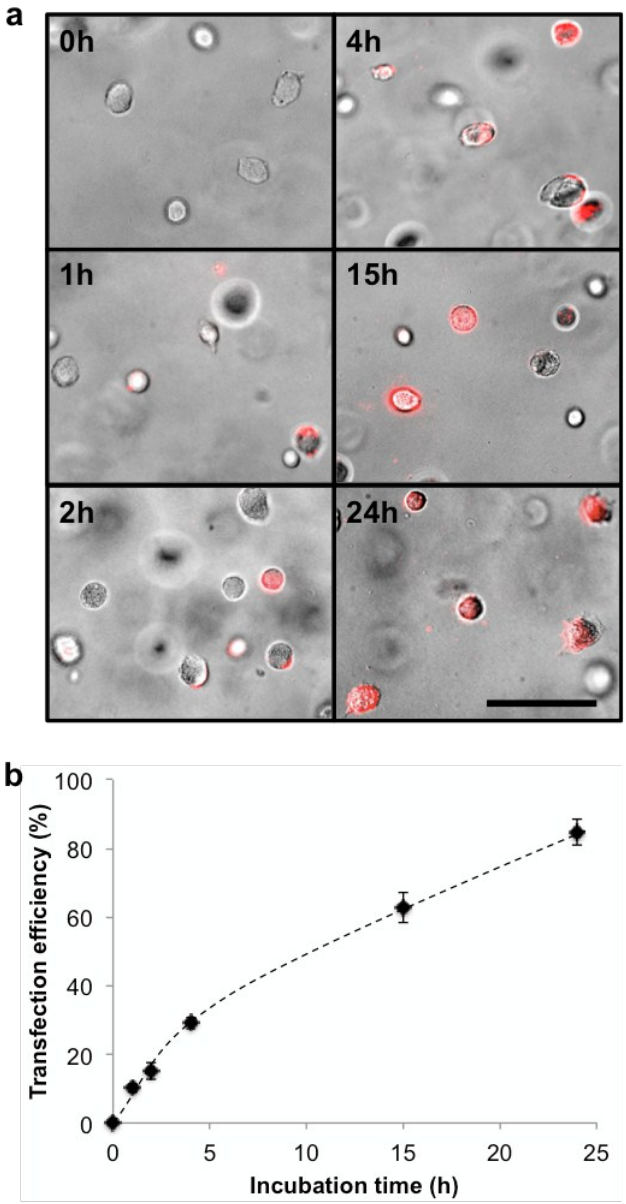

Figure 6. Cellular uptake of CaP/Cy3-siRNA/Gln-OChi in 3D hydrogel system. ADSCs were encapsulated in the photocrosslinkable chitosan hydrogel with CaP/Cy3-siRNA/Gln-OChi and incubated for 24 h. a) Merged images of bright field images for encapsulated ADSCs and fluorescent images for CaP/Cy3-siRNA/Gln-OChi. Scale bar is 100 µm. b) Transfection efficiency (%) of CaP/Cy3-siRNA/Gln-OChi into ADSCs in 3D hydrogel was analyzed as a function of time by counting transfected cells in relation to the total number of cells (n = 5).

examined by qRT-PCR analysis (Figure 7a). Lipofectamine® 2000 was used as a positive control. After 3 days in culture, mRNA level of NOG was significantly decreased to 49% and 45% in the hydrogels containing CaP/Gln-OChi and Lipofectamine® 2000, respectively, whereas no significant change was observed in the hydrogels containing naked siNOG, blank NPs without siRNA, or NPs with control-siRNA. The osteogenic effect of NOG suppression was evaluated by ALP expression in ADSCs (Figure 7b). Our results showed that ADSCs incubated with siNOG-loaded CaP/Gln-OChi NP significantly increased

Journal of Materials Chemistry B Accepted Manuscript

This journal is © The Royal Society of Chemistry 20xx

Please do not adjust margins

expression of ALP to the similar extent to Lipofectamine®-mediated ALP expression. ALP expression was further confirmed by ALP staining as shown in Figure 7c. Live/Dead staining showed a high level of viability of encapsulated cells (>90%) during transfection in the hydrogel (Figure 7d). The collective results indicate that CaP/Gln-OChi NPs not only successfully delivered siNOG into primary ADSCs but also suppressed the expression of target gene (NOG), which induced osteogenic differentiation of encapsulated cells in 3D hydrogel environment.

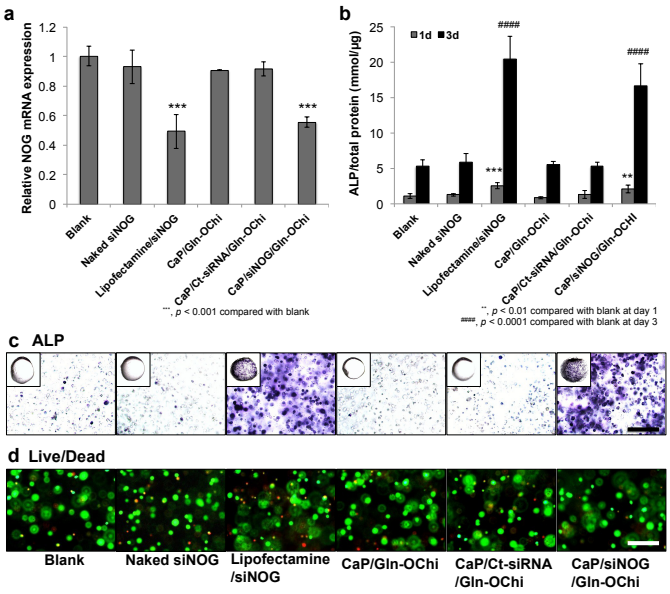

Figure 7. Effect of NOG knockdown by NPs on osteogenic differentiation in 3D hydrogel system. a) qRT-PCR quantification of NOG mRNA expression after 3 days in culture. b) Quantitative assay for ALP activity of ADSCs at day 1 and day 3. ALP activities were normalized by total protein contents. c) ALP staining was evaluated by light microscopy after 3 days of osteogenic differentiation. Differentiated cells positive for ALP were stained blue. Images are representative of a total analysis of three samples. d) In vitro viability of ADSCs in 3D hydrogels was assessed using the Live/Dead staining after 3 days in culture. Scale bars are 200 μm.

Conclusions

The formation of CaP NPs was stabilized via Gln-conjugated chitosan (Gln-OChi) coating which introduced electrostatically stable (> +30 mV) particles without aggregation. Gln-OChi coating significantly enhanced the transfection efficiency of the NPs in both immortalized cell line and primary cells with no significant cytotoxicity. Moreover, the Gln-OChi coated CaP NPs loaded with siRNA targeting BMP antagonist NOG greatly suppressed the expression of NOG in MSCs and subsequently enhanced their osteogenic differentiation in in vitro 3D hydrogel microenvironments. These results indicate that our nanocarrier system prepared with synthetic bone mineral and natural polysaccharide may be an effective and safe vehicle for therapeutic drug/gene delivery.

Acknowledgements

This work was supported by the National Institutes of Health grants R01 AR060213 and R21 DE021819, the International Association for Dental Research, and the Academy of Osseointegration.

Notes and references

1. A. K. Pannier and L. D. Shea, *Mol. Ther.*, 2004, **10**, 19-26.
2. T. R. Flotte, *J. Cell. Physiol.*, 2007, **213**, 301-305.
3. T. Niidome and L. Huang, *Gene Ther.*, 2002, **9**, 1647-1652.
4. Y. K. Oh and T. G. Park, *Adv. Drug Deliv. Rev.*, 2009, **61**, 850-862.
5. H. J. Park, J. Shin, J. Kim and S. W. Cho, *Arch. Pharm. Res.*, 2014, **37**, 107-119.
6. S. M. Elbashir, J. Harborth, W. Lendeckel, A. Yalcin, K. Weber and T. Tuschl, *Nature*, 2001, **411**, 494-498.
7. D. Bumcrot, M. Manoharan, V. Koteliansky and D. W. Sah, *Nat. Chem. Biol.*, 2006, **2**, 711-719.
8. A. J. Mellott, M. L. Forrest and M. S. Detamore, *Ann. Biomed. Eng.*, 2013, **41**, 446-468.
9. O. Gresch, F. B. Engel, D. Nesic, T. T. Tran, H. M. England, E. S. Hickman, I. Korner, L. Gan, S. Chen, S. Castro-Obregon, R. Hammermann, J. Wolf, H. Muller-Hartmann, M. Nix, G. Siebenkotten, G. Kraus and K. Lun, *Methods*, 2004, **33**, 151-163.
10. Z.-K. Cui and M. Lafleur, *Colloid Surf. B-Biointerfaces*, 2014, **114**, 177-185.
11. S. Stender, M. Murphy, T. O'Brien, C. Stengaard, M. Ulrich-Vinther, K. Soballe and F. Barry, *Eur. Cell. Mater.*, 2007, **13**, 93-99; discussion 99.
12. C. E. Thomas, A. Ehrhardt and M. A. Kay, *Nat. Rev. Genet.*, 2003, **4**, 346-358.
13. H. J. Park, F. Yang and S. W. Cho, *Adv. Drug Deliv. Rev.*, 2012, **64**, 40-52.
14. T. Liu, A. Tang, G. Zhang, Y. Chen, J. Zhang, S. Peng and Z. Cai, *Cancer Biother. Radiopharm.*, 2005, **20**, 141-149.
15. V. V. Sokolova, I. Radtke, R. Heumann and M. Epple, *Biomaterials*, 2006, **27**, 3147-3153.
16. V. Sokolova and M. Epple, *Angew. Chem. Int. Ed. Engl.*, 2008, **47**, 1382-1395.
17. F. L. Graham and A. J. van der Eb, *Virology*, 1973, **52**, 456-467.
18. M. Jordan, A. Schallhorn and F. M. Wurm, *Nucleic Acids Res.*, 1996, **24**, 596-601.
19. M. Jordan and F. Wurm, *Methods*, 2004, **33**, 136-143.
20. I. Roy, S. Mitra, A. Maitra and S. Mozumdar, *Int. J. Pharm.*, 2003, **250**, 25-33.
21. S. Bisht, G. Bhakta, S. Mitra and A. Maitra, *Int. J. Pharm.*, 2005, **288**, 157-168.
22. F. Pittella, H. Cabral, Y. Maeda, P. Mi, S. Watanabe, H. Takemoto, H. J. Kim, N. Nishiyama, K. Miyata and K. Kataoka, *J. Control. Release*, 2014, **178**, 18-24.
23. A. Maitra, *Expert Rev. Mol. Diagn.*, 2005, **5**, 893-905.
24. X. Cao, W. Deng, R. Qu, Q. Yu, J. Li, Y. Yang, Y. Cao, X. Gao, X. Xu and J. Yu, *Adv. Funct. Mater.*, 2013, **23**, 5403-5411.
25. M. S. Lee, J. E. Lee, E. Byun, N. W. Kim, K. Lee, H. Lee, S. J. Sim, D. S. Lee and J. H. Jeong, *J. Control. Release*, 2014, **192**, 122-130.

Journal of Materials Chemistry B Accepted Manuscript

Please do not adjust margins

26. M. F. Pittenger, A. M. Mackay, S. C. Beck, R. K. Jaiswal, R. Douglas, J. D. Mosca, M. A. Moorman, D. W. Simonetti, S. Craig and D. R. Marshak, *Science*, 1999, **284**, 143-147.
27. S. M. Richardson, J. A. Hoyland, R. Mobasheri, C. Csaki, M. Shakibaei and A. Mobasheri, *J. Cell. Physiol.*, 2010, **222**, 23-32.
28. M. Al-Nbaheen, R. Vishnubalaji, D. Ali, A. Bouslimi, F. Al-Jassir, M. Megges, A. Prigione, J. Adjaye, M. Kassem and A. Aldahmash, *Stem Cell Rev. Rep.*, 2013, **9**, 32-43.
29. A. Mukerjee, J. Shankardas, A. P. Ranjan and J. K. Vishwanatha, *Nanotechnol.*, 2011, **22**, 445101.
30. J. L. Santos, D. Pandita, J. Rodrigues, A. P. Pego, P. L. Granja and H. Tomas, *Curr. Gene Ther.*, 2011, **11**, 46-57.
31. A. Hamm, N. Krott, I. Breibach, R. Blindt and A. K. Bosserhoff, *Tissue Eng.*, 2002, **8**, 235-245.
32. J. K. F. Suh and H. W. T. Matthew, *Biomaterials*, 2000, **21**, 2589-2598.
33. A. Di Martino, M. Sittinger and M. V. Risbud, *Biomaterials*, 2005, **26**, 5983-5990.
34. E. Khor and L. Y. Lim, *Biomaterials*, 2003, **24**, 2339-2349.
35. H. Gao, W. Shi and L. B. Freund, *Proc. Natl. Acad. Sci. U. S. A.*, 2005, **102**, 9469-9474.
36. C. He, Y. Hu, L. Yin, C. Tang and C. Yin, *Biomaterials*, 2010, **31**, 3657-3666.
37. J. Cao, X. Xie, A. Lu, B. He, Y. Chen, Z. Gu and X. Luo, *Biomaterials*, 2014, **35**, 4517-4524.
38. V. Torchilin, *Adv. Drug Deliv. Rev.*, 2011, **63**, 131-135.
39. M. R. Rekha and C. P. Sharma, *J. Appl. Polym. Sci.*, 2011, **122**, 2374-2382.
40. F. Pittella, M. Zhang, Y. Lee, H. J. Kim, T. Tockary, K. Osada, T. Ishii, K. Miyata, N. Nishiyama and K. Kataoka, *Biomaterials*, 2011, **32**, 3106-3114.
41. S. Park, E. J. Jeong, J. Lee, T. Rhim, S. K. Lee and K. Y. Lee, *Carbohydr. Polym.*, 2013, **92**, 57-62.
42. D. W. Lee, K. S. Yun, H. S. Ban, W. Choe, S. K. Lee and K. Y. Lee, *J. Control. Release*, 2009, **139**, 146-152.
43. B. T. Estes, B. O. Diekman, J. M. Gimble and F. Guilak, *Nat. Protoc.*, 2010, **5**, 1294-1311.
44. J. Fan, H. Park, M. Lee, O. Bezouglaia, A. Fartash, J. Kim, T. Aghaloo and M. Lee, *Tissue Eng. Part A*, 2014, **20**, 2169-2179.
45. T. Luhmann, M. Rimann, A. G. Bittermann and H. Hall, *Bioconjug. Chem.*, 2008, **19**, 1907-1916.
46. J. Hu, Y. Hou, H. Park, B. Choi, S. Hou, A. Chung and M. Lee, *Acta Biomater.*, 2012, **8**, 1730-1738.
47. C. Yu, S. Young, V. Russo, B. G. Amsden and L. E. Flynn, *Tissue Eng. Part C*, 2013, **19**, 829-838.
48. J. B. Fan, H. Park, S. Tan and M. Lee, *PLoS One*, 2013, **8**, e72474.
49. S. Prabha, W. Z. Zhou, J. Panyam and V. Labhasetwar, *Int. J. Pharm.*, 2002, **244**, 105-115.
50. R. H. Müller, *Zetapotential und Partikelladung in der Laborpraxis*, Wissenschaftliche Verlagsges, 1996.
51. Y. Li, L. Cui, Q. Li, L. Jia, Y. Xu, Q. Fang and A. Cao, *Biomacromolecules*, 2007, **8**, 1409-1416.
52. M. Liu, B. Chen, Y. Xue, J. Huang, L. Zhang, S. Huang, Q. Li and Z. Zhang, *Bioconjug. Chem.*, 2011, **22**, 2237-2243.
53. L. Casettari, D. Vllasaliu, J. K. Lam, M. Soliman and L. Illum, *Biomaterials*, 2012, **33**, 7565-7583.
54. M. Thibault, S. Nimesh, M. Lavertu and M. D. Buschmann, *Mol. Ther.*, 2010, **18**, 1787-1795.
55. J. Malmo, H. Sorgard, K. M. Varum and S. P. Strand, *J. Control. Release*, 2012, **158**, 261-268.
56. H. Park, B. Choi, J. Hu and M. Lee, *Acta Biomater.*, 2013, **9**, 4779-4786.
57. C. Arakawa, R. Ng, S. Tan, S. Kim, B. Wu and M. Lee, *J. Tissue Eng. Regen. Med.*, 2014, DOI: 10.1002/term.1896.
58. S. M. Warren, L. J. Brunet, R. M. Harland, A. N. Economides and M. T. Longaker, *Nature*, 2003, **422**, 625-629.
59. J. Groppe, J. Greenwald, E. Wiater, J. Rodriguez-Leon, A. N. Economides, W. Kwiatkowski, M. Affolter, W. W. Vale, J. C. Belmonte and S. Choe, *Nature*, 2002, **420**, 636-642.
60. W. C. Smith and R. M. Harland, *Cell*, 1992, **70**, 829-840.

Journal of Materials Chemistry B Accepted Manuscript

This journal is © The Royal Society of Chemistry 20xx

Please do not adjust margins

CaP nanoparticles coated with highly cationic, glutamine-conjugated oligochitosan (Gln-OChi) are developed for siRNA delivery to significantly enhance gene transfection and knockdown efficiency with minimal cytotoxicity. The osteogenic bioactivity of siRNA delivered by CaP/Gln-OChi particles has been elevated in three-dimensional environments by using photocrosslinkable chitosan hydrogels encapsulating stem cells. Our CaP/Gln-OChi nanocarrier can potentially be used for gene therapy.

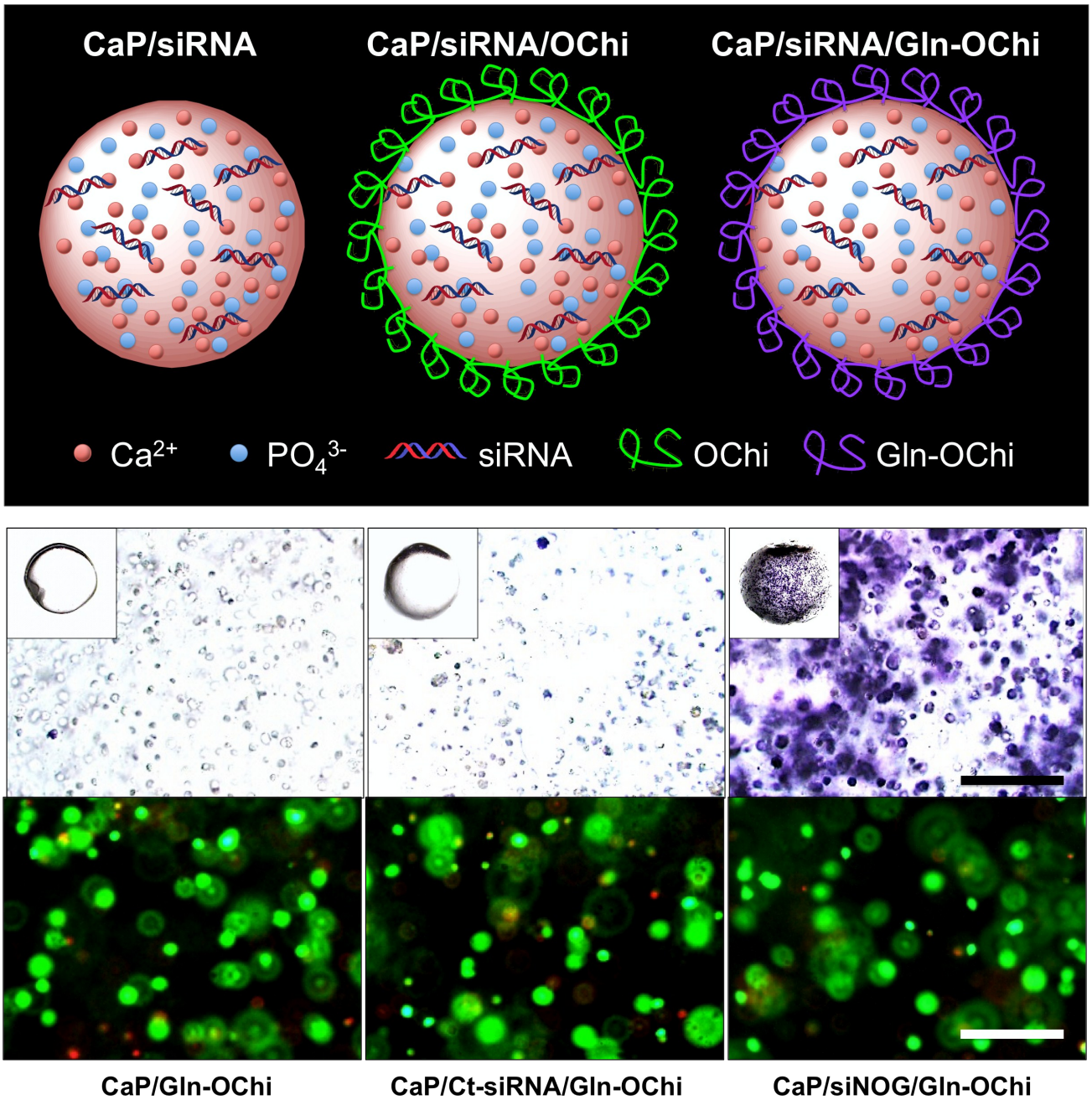

Journal of Materials Chemistry B Accepted Manuscript